AGU PUBLICATIONS

JGR

Journal of Geophysical Research: Atmospheres

RESEARCH ARTICLE
10.1002/2016JD025832

Corona discharges from a windmill and its lightning protection tower in winter thunderstorms

Ting Wu[1], Daohong Wang[1], William Rison[2], Ronald J. Thomas[2], Harald E. Edens[2], Nobuyuki Takagi[1], and Paul R. Krehbiel[2]

[1]Department of Electrical, Electronic and Computer Engineering, Gifu University, Gifu, Japan, [2]Langmuir Laboratory for Atmospheric Research, Geophysical Research Center, New Mexico Institute of Mining and Technology, Socorro, New Mexico, USA

Key Points:
- Windmill coronas radiate larger power and possibly develop to higher altitudes than tower coronas do
- Windmill corona production is periodic, but only two out of three blades of the windmill produce detectable radiation
- Coronas are not related with upward leader initiation, but nearby lightning can increase corona production rates right after the flash

Correspondence to:
T. Wu,
tingwu@gifu-u.ac.jp

Citation:
Wu, T., D. Wang, W. Rison, R. J. Thomas, H. E. Edens, N. Takagi, and P. R. Krehbiel (2017), Corona discharges from a windmill and its lightning protection tower in winter thunderstorms, *J. Geophys. Res. Atmos.*, *122*, 4849–4865, doi:10.1002/2016JD025832.

Received 24 AUG 2016
Accepted 11 APR 2017
Accepted article online 18 APR 2017
Published online 8 MAY 2017
Corrected 16 JUN 2017

This article was corrected on 16 JUN 2017. See the end of the full text for details.

Abstract This paper presents lightning mapping array (LMA) observations of corona discharges from a windmill and its lightning protection tower in winter thunderstorms in Japan. Corona discharges from the windmill, called windmill coronas, and those from the tower, called tower coronas, are distinctly different. Windmill coronas occur with periodic bursts, generally radiate larger power, and possibly develop to higher altitudes than tower coronas do. A strong negative electric field is necessary for the frequent production of tower coronas but is not apparently related with windmill coronas. These differences are due to the periodic rotation of the windmill and the moving blades which can escape space charges produced by corona discharges and sustain a large local electric field. The production period of windmill coronas is related with the rotation period of the windmill. Surprisingly, for one rotation of the windmill, only two out of the three blades produce detectable discharges and source powers of discharges from these two blades are different. The reason for this phenomenon is still unclear. For tower coronas, the source rate can get very high only when there is a strong negative electric field, and the source power can get very high only when the source rate is very low. The relationship between corona discharges and lightning flashes is investigated. There is no direct evidence that corona discharges can increase the chance of upward leader initiation, but nearby lightning flashes can increase the source rate of corona discharges right after the flashes. The peak of the source height distribution of corona discharges is about 100 m higher than the top of the windmill and the top of the tower. Possible reasons for this result are discussed.

1. Introduction

It is well known that in the enhanced electric field under thunderstorms, pointed objects on the ground such as towers, trees, and grass can produce corona discharges. Corona discharges are confined in a small region around conductive points where the electric field is larger than that necessary for electrical breakdown. Corona discharges produce space charges in front of the electrode, which shield the electrode and decrease the local electric field. However, if the ambient electric field is strong enough and there are large quantities of space charges, the electric field produced by the space charges can generate further ionization and result in weakly conducting streamer channels. If the ambient electric field keeps growing, the current of streamers can get large enough to heat the streamer stem and turn it into a hot, conducting, and self-propagating leader channel [*Cooray*, 2015].

Corona discharges also emit electromagnetic radiation but are much less powerful than lightning discharges. As a result, direct observations of corona discharges under thunderstorms are quite scarce and most studies about corona discharges are carried out by laboratory experiment [e.g., *Waters*, 1975] and numerical simulation [e.g., *Becerra et al.*, 2007]. Early studies also paid attention to the influence of space charges produced by corona discharges on the electric field under thunderstorms [*Toland and Vonnegut*, 1977; *Standler and Winn*, 1979; *Soula and Chauzy*, 1991]. Recently, *Montanya et al.* [2014] and *Rison et al.* [2015] both successfully observed corona discharges from windmills using the lightning mapping array (LMA). *Montanya et al.* [2014] reported observation of periodic corona discharges at regular intervals of about 3.15 s from a windmill in Spain. Most detected VHF radiation sources were below 2 km in altitude and had powers of about −5 dBW. *Rison et al.* [2015] made a similar observation in a wind farm in Kansas. They found that the period

of corona discharge groups was the same as the rotation period of the windmill, indicating that only one out of the three blades produced detectable discharges. They also found that the altitude of the corona sources centered between the hub of the windmill and the blade tips.

During the winter campaign in 2014, we set up a nine-station LMA around a windmill and its lightning protection tower in Uchinada, Japan [*Wang et al.*, 2015]. We have been making winter lightning observation for many years, mainly using high-speed optical systems supplemented with electric field mills, and fast and slow antennas [*Wang et al.*, 2008; *Wang and Takagi*, 2012]. This is the first time that LMA has been used for winter lightning observation in Japan. Winter lightning in Japan has many special characteristics including a high percentage of positive cloud-to-ground flashes [e.g., *Takeuti et al.*, 1978], frequent bipolar flashes [e.g., *Narita et al.*, 1989] and upward flashes [e.g., *Wang et al.*, 2008], a very small time difference between preliminary breakdown and the return stroke [*Brook*, 1992; *Wu et al.*, 2013], and some discharge processes that have not been observed in summer thunderstorms [*Wu et al.*, 2014]. With the help of LMA, we intend to further investigate the initiation and propagation characteristics of upward and bipolar flashes, and the relationship between lightning types and the charge structure of winter thunderstorms. An analysis of the LMA data showed that the system was triggered most frequently by corona discharges. As a first report, this paper will describe the observation of corona discharges from a windmill and its lightning protection tower. We will describe different characteristics of corona discharges from the windmill and the tower and investigate possible relationships between corona discharges and lightning flashes. Based on the observation results, we will discuss the physical processes responsible for the observed corona discharges.

2. Experiment and Data

During the winter of 2014, a nine-station LMA was deployed near the Japan Sea coast in the Hokuriku region where winter lightning frequently occurs. LMA is a widely used lightning location system working in the VHF band [*Rison et al.*, 1999]. It can accurately locate sources of VHF radiation of basically all types of lightning discharges. Figure 1a shows the array. It covers an area of about 18×18 km^2, forming a compact network, which is capable of detecting discharges with very weak radiation, such as corona discharges. A windmill is located at (0, 0), and its lightning protection tower is about 45 m away. The ground level is about 50 m. The height of the windmill (from the base to the tip of a blade pointing upward) is 100 m, and the height of the tower is 105 m. So the altitude of the tower top is 155 m and the maximum altitude of the windmill is 150 m. Details of the tower and the windmill are also described by *Wang and Takagi* [2012].

From Figure 1a we can see that all sources of corona discharges are located near the windmill and the tower (at this scale, we cannot differentiate the windmill and the tower from corona sources). An enlarged image for the region near the windmill is shown in Figure 1b. Most of the sources are centered around the windmill and the tower. Sources around the windmill seem to have higher power than those around the tower. Overall, the source power of corona discharges is quite low, mainly below −10 dBW (about 0.1 W). This is compared to source powers from 0 dBW up to 40 dBW for normal intracloud discharges [*Thomas et al.*, 2001].

Corona discharges analyzed in this paper are observed in two periods: 15:00–21:00, 14 November and 13:50–23:00, 2 December 2014 (universal time). In these two periods, the LMA was operated continuously without any trouble, and a large number of corona discharge sources were located. Figures 1c and 1d show the time series of corona discharges in these two periods. Most of the sources were lower than 600 m. During some short periods, some sources reached about 1000 m.

Figure 2 shows height distributions of all corona sources on 14 November and 2 December. It also shows the ground level, the top of the tower, and the top of the windmill. We can see a predominant peak at 50–60 m on both days. At first, we thought this peak was produced by corona discharges on the ground. However, LMA in this study does not seem to be able to detect corona discharges on the ground. During this observation, almost all corona discharges are located at the tower and the windmill. If this peak was produced by corona discharges on the ground, there should have been corona discharges detected everywhere inside the array. It seems that LMA is only capable of detecting relatively strong corona discharges from tall objects, and all sources in Figure 2 should be produced from the tower and the windmill. Figure 2c shows the distribution of reduced chi-square values (χ_v^2) versus heights for all corona discharge sources. As discussed by *Thomas et al.* [2004], χ_v^2 is an indication of the location error, and we are only using location results with χ_v^2 smaller than 5.

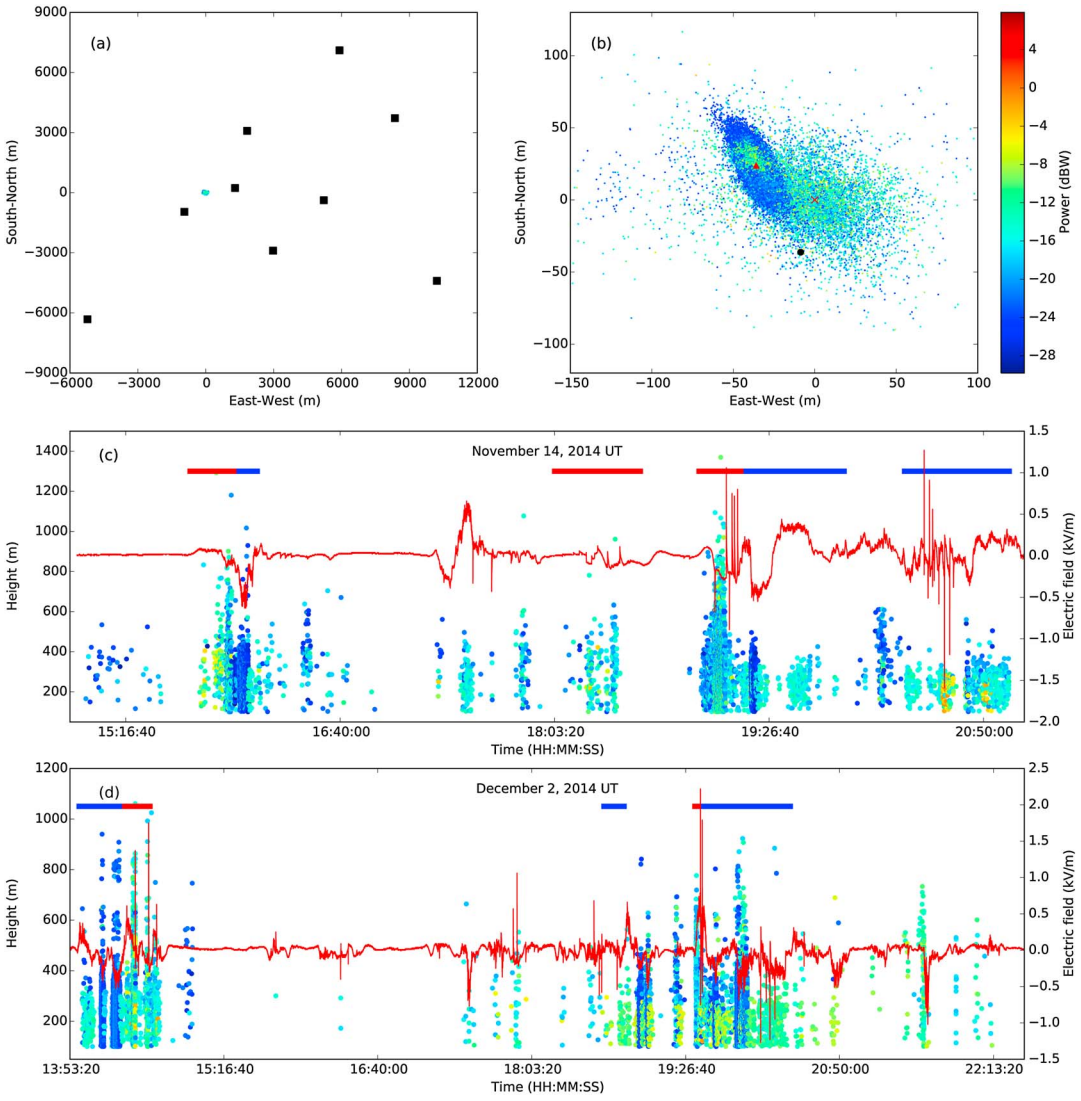

Figure 1. Sources of corona discharges located by the LMA. (a) Network of LMA. All sources of corona discharges are located near the windmill (0, 0) and a nearby tower. (b) Locations of corona discharges and the windmill (red cross), the tower (red triangle), and the field mill (black dot). (c) Time sequence of source height of corona discharges on 14 November. Red curve represents electric field. Red and blue horizontal lines indicate periods of windmill coronas and tower coronas, respectively. (d) The same as Figure 1c but for 2 December. Source color indicates radiation power determined by LMA.

From Figure 2 we can see that many sources near the ground have relatively large errors, also indicating that sources near the ground may be not real and were caused by location errors. The large number of sources mislocated near the ground may pose a significant influence on the analysis, so we decided that only sources above 100 m (black dashed lines in Figure 2) are used in this study.

The electric field measured by an electric field mill near the windmill is also shown in Figures 1c and 1d. The field mill has a sampling rate of 20 samples/s, shown as a black dot in Figure 1b. Due to the shielding effect of the windmill, the absolute value of the electric field strength is underestimated. Atmospheric sign convention is used for the electric field record, so a positive value indicates a downward electric field.

We also have high-speed video recordings of lightning flashes striking at the windmill and the tower. These data will not be analyzed in detail in this paper but will only be used to determine striking locations for some flashes of interest.

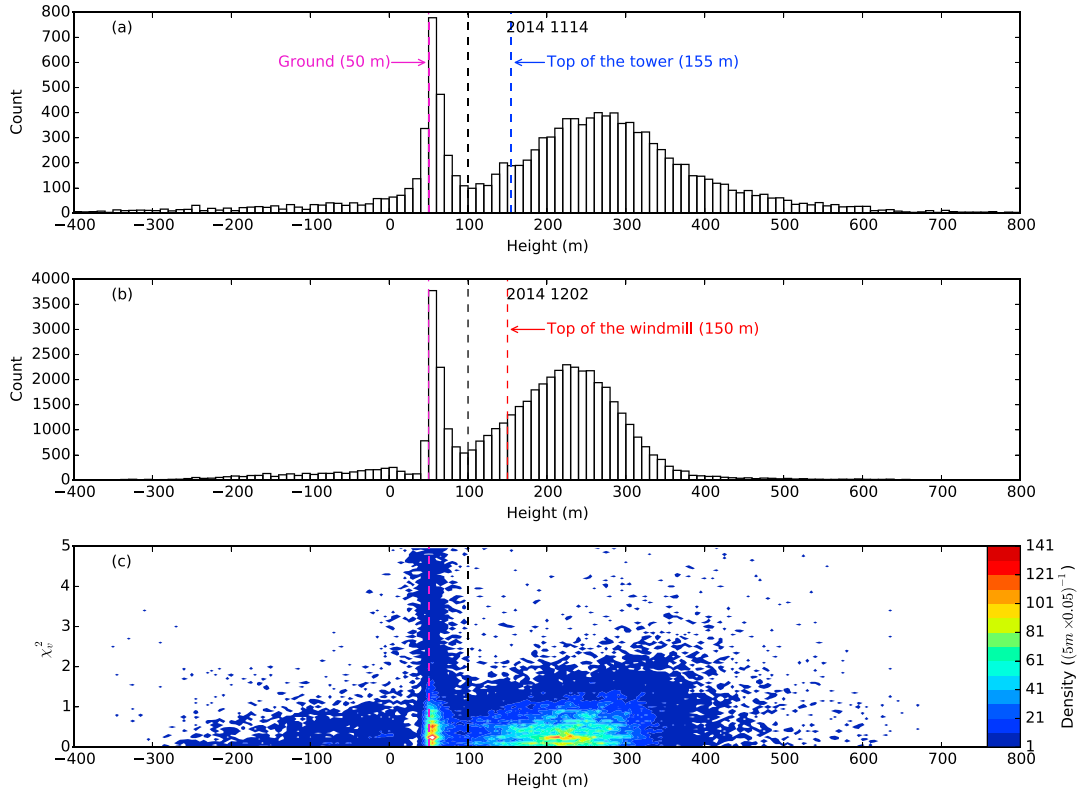

Figure 2. Height distribution of all corona sources on (a) 14 November and (b) 2 December. (c) Reduced chi-square values (χ^2_ν) versus sources heights. Color indicates the source density. Purple dashed lines indicate the ground level. Blue dashed line in Figure 2a indicates the top altitude of the tower. Red dashed line in Figure 2b indicates the top altitude of the windmill. Black dashed lines indicate the height of 100 m, sources below which are not analyzed in this study.

3. Results

3.1. Two Types of Corona Discharges

From Figure 1b we have already noticed that corona discharges from the windmill and the tower have quite different powers. The tower is at least 5 m taller than the windmill and has a sharper top (there is a lightning rod at the top of the tower), so when the windmill is not rotating, corona discharges are more likely to be produced from the tower. However, when the windmill is rotating, the moving blade is capable of escaping the space charges produced by corona discharges and is likely to produce corona discharges more frequently. Due to the fundamental difference between the tower and the windmill, more differences in their corona discharges are expected. In this section, we will explore the differences between corona discharges from the tower and the windmill.

For this analysis, we need to first classify all corona discharges into those from the tower and those from the windmill. If we knew the periods when the windmill was or was not rotating, the classification would be very easy. Unfortunately, we could not get this information from the windmill operator. As a result, we can only make the classification based on source locations. We carefully checked source locations of all corona discharges and found some periods during which sources were predominantly occurring near the tower (blue horizontal lines in Figures 1c and 1d) and some periods during which sources were predominantly occurring near the windmill (red horizontal lines in Figures 1c and 1d). In other periods, we were unable to determine whether the tower or the windmill was playing a predominant role in producing the sources. In the following analyses, we will refer to corona discharges occurring around the windmill as windmill coronas and those around the tower as tower coronas. It should be noted that this classification is not strict; periods of windmill corona may also include a small number of tower coronas and vice versa. This is unavoidable as the tower and the windmill are closely situated and will always have certain effects on the production of corona discharges. We have tried to select the periods during which most of the sources are clearly produced by either the tower

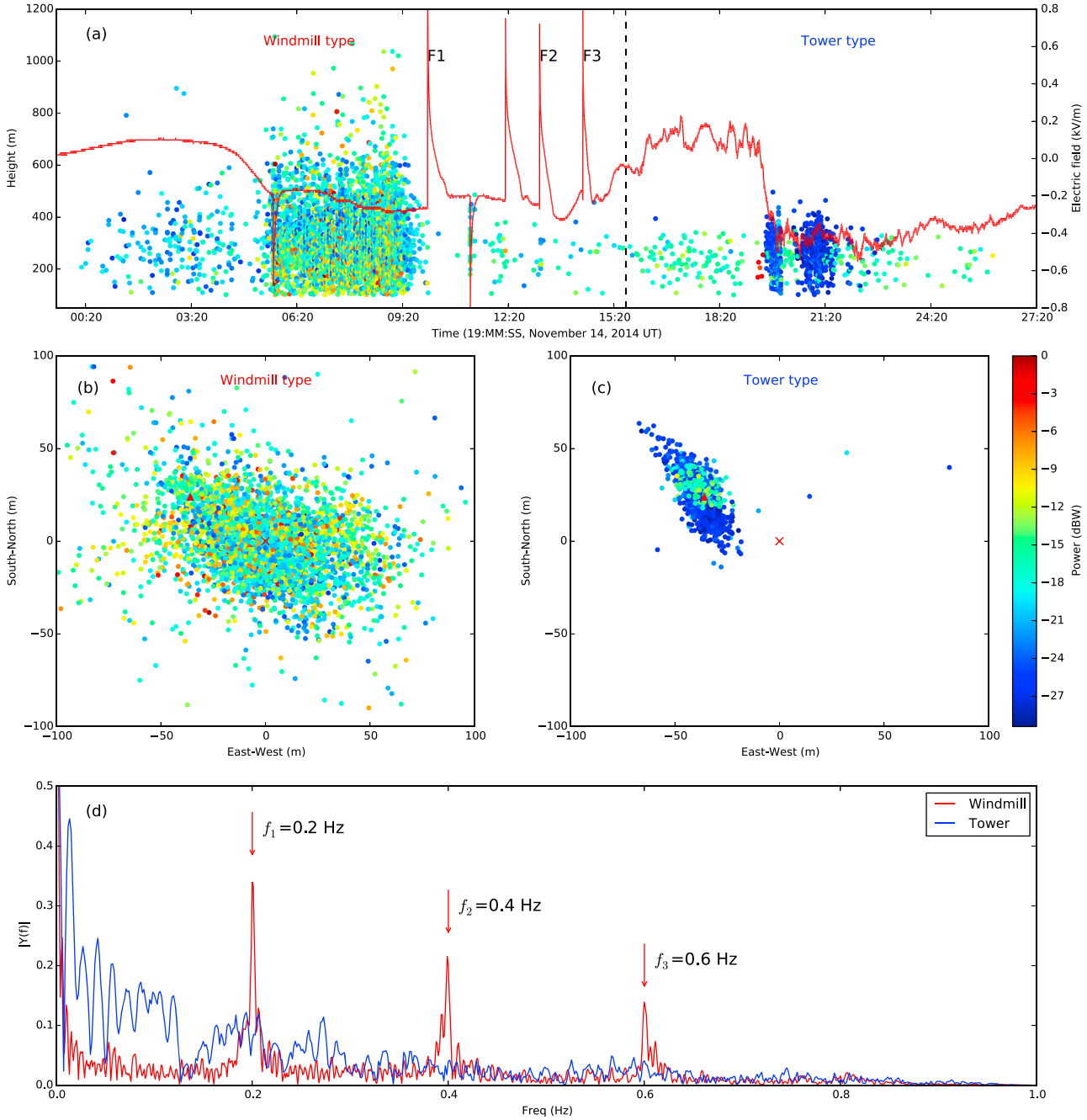

Figure 3. A short period on 14 November during which a large number of windmill coronas occurred, followed by tower coronas. (a) Time series of source height and electric field. F1–F3 indicates the time when upward lightning flashes occurred. Sources of these flashes are not plotted. (b) Locations of windmill coronas with respect to the windmill and tower. (c) Locations of tower coronas with respect to the windmill and tower. (d) Production frequency of sources of windmill coronas and tower coronas.

or the windmill. Two of the periods are shown in detail in Figures 3 and 4, and the statistical results for all selected periods will be analyzed in this section.

Figure 3 shows a segment of 28 min on 14 November (also shown in Figure 1c), during which a large number of windmill coronas are followed by a large number of tower coronas. A black dashed line in Figure 3a divides windmill coronas and tower coronas.

Figure 3b shows locations of windmill coronas (before the black dashed line), which are centered around the windmill. Although some sources are located around the tower, we cannot see clearly the contribution of the

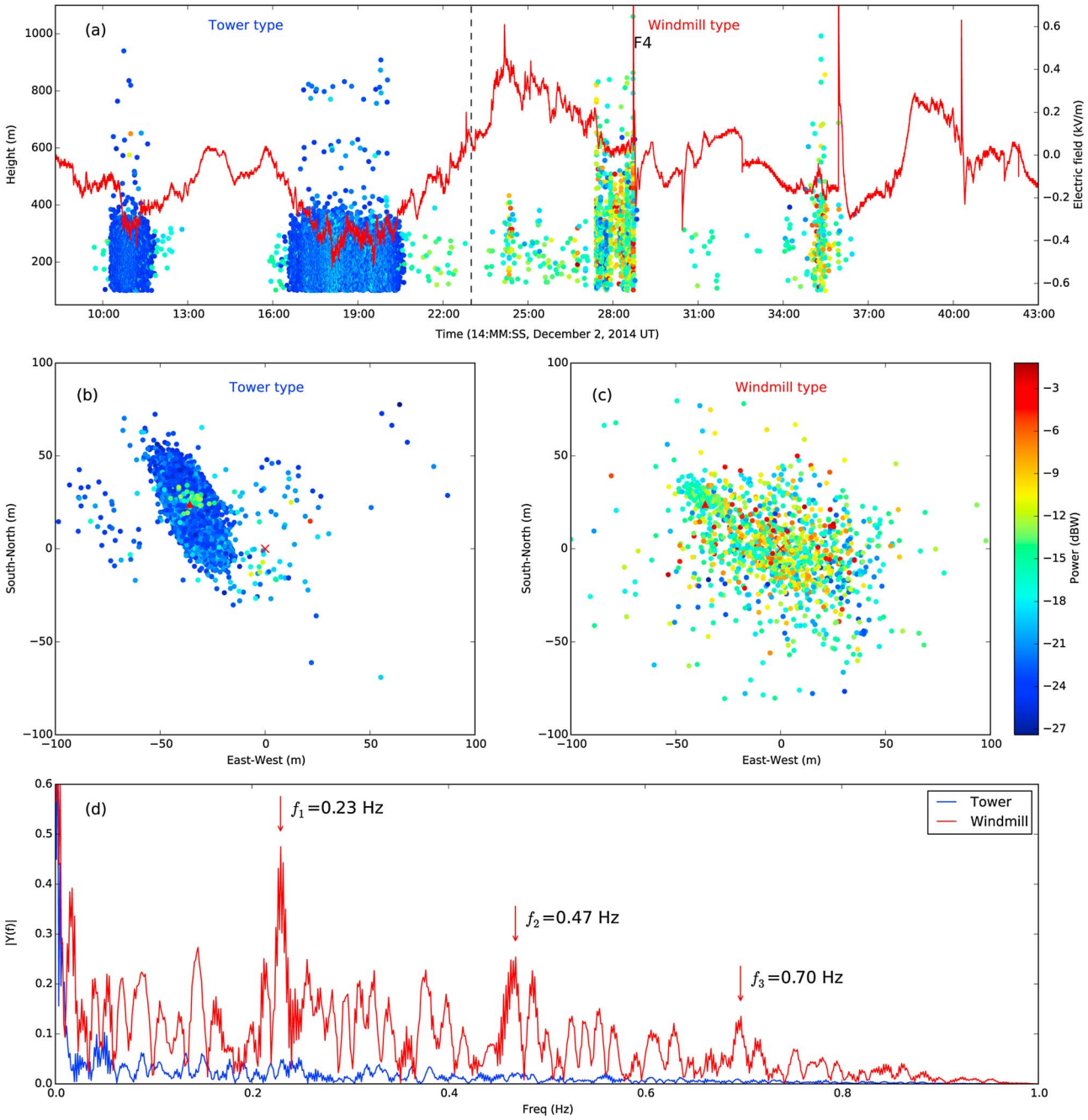

Figure 4. The same as Figure 3 but for a period on 2 December.

tower to the production of these sources. By comparison, Figure 3c shows locations of tower coronas (after the black dashed line), which are centered around the tower. Almost no sources are located near the windmill. It seems that the majority of sources in Figure 3c are produced from the tower. An obvious difference between the two types of discharges is that sources of windmill coronas are generally more powerful.

Figure 3d shows the frequency distribution of source production for the two types of discharges. The frequency is calculated by first counting source numbers in every 0.1 s segment and then performing the Fourier transform. The frequency for windmill coronas shows three clear peaks, at 0.2, 0.4, and 0.6 Hz, while the frequency for tower coronas does not show any clear peak. It clearly indicates the effect of the windmill rotation on the production of windmill coronas.

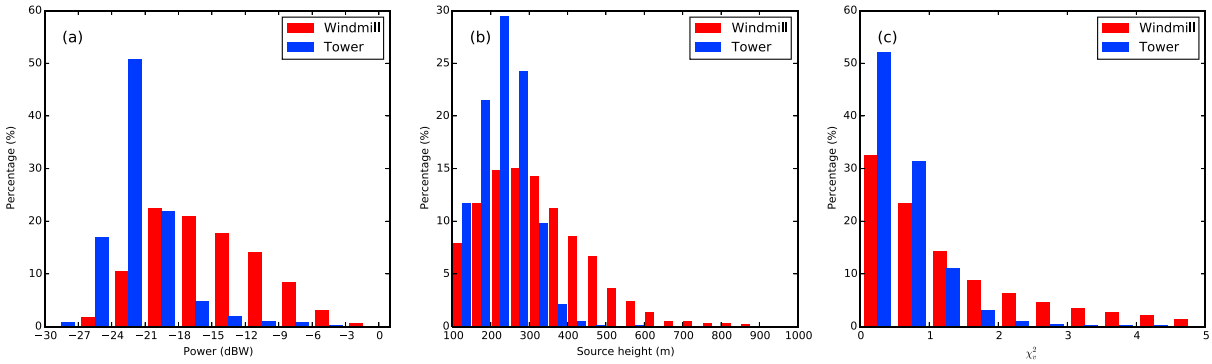

Figure 5. Comparison of windmill coronas and tower coronas. (a) Distribution of source power. (b) Distribution of source altitude. (c) Distribution of reduced chi-square value (χ_v^2).

Figure 4 shows a segment of 34 min on 2 December (also shown in Figure 1d). During this period, a large number of tower coronas are followed by windmill coronas. Figure 4b shows the locations of tower coronas (before the black dashed line). The majority of sources are located around the tower. A few sources are scattered, but it seems that the windmill has little contribution to the production of these sources. Figure 4c shows the locations of windmill coronas (after the black dashed line). In this case, the sources are scattered around the windmill. Some sources (green ones near the tower) seem to be produced from the tower. It looks like they were produced alongside with the corona discharges from the windmill. As is the case in Figure 3, sources of windmill coronas are generally more powerful than tower coronas.

Figure 4d shows source production frequencies. The frequency for tower coronas still does not have any clear peak, similar to the case in Figure 3. The frequency for windmill coronas shows some peaks but not very clear. However, we can still identify three frequency components as indicated by three arrows in Figure 4d. The f_2 is about 2 times of f_1, and f_3 is about 3 times of f_1, the same as the case in Figure 3. The values of the frequencies are different, indicating that the rotation speed of the windmill was different.

Based on the above two cases, differences between windmill coronas and tower coronas are further analyzed and summarized as follows.

1. Windmill coronas generally have larger powers than tower coronas. From the Figures 3b, 3c, 4b, and 4c we can see that sources of windmill coronas are much more powerful than those of tower coronas. Figure 5a shows source power distributions for the two types of discharges in all selected periods (as indicated in Figure 1). The source power of tower coronas centers in −27 to −18 dBW while the source power of windmill coronas has a wide distribution from −24 to −6 dBW. The average values are −21.7 and −15.5 dBW, respectively, for tower coronas and windmill coronas. The smallest source power that could be detected in the observation by *Rison et al.* [2015] was −20 dBW, and they only detected one short period of corona discharges from towers. The typical source power detected in the observation by *Montanya et al.* [2014] was about −5 dBW, and apparently, they did not detect any corona discharges from towers or other stationary objects. These results also indicate that the power of windmill coronas is stronger than that of tower coronas.
2. Sources of windmill coronas can reach higher altitudes than those of tower coronas. From the Figures 3a and 4a, we can see that most of the sources of tower coronas are below 400 m, while for windmill coronas a significant portion of the sources are between 400 and 600 m. Figure 5b shows the distribution of source altitudes for two types of discharges in all selected periods (as indicated in Figure 1). The distribution for windmill coronas is much wider, with a much higher percentage of sources reaching altitudes above 400 m. The average values are 230.5 and 321.0 m, respectively, for tower coronas and windmill coronas. It should be noted that sources below 100 m are not used for this analysis, so these average values may be overestimated. As shown in Figure 5c, windmill coronas also have a wider distribution of χ_v^2, indicating that location errors for windmill coronas are larger, and it is possible that the height difference between tower and windmill coronas are due to different location errors. More will be discussed on this issue in section 4.2.
3. The production of windmill coronas shows three characteristic frequency components: f_1, f_2, and f_3, in which $f_2 = 2f_1$ and $f_3 = 3f_1$. These frequency components are caused by the periodic rotation of the windmill,

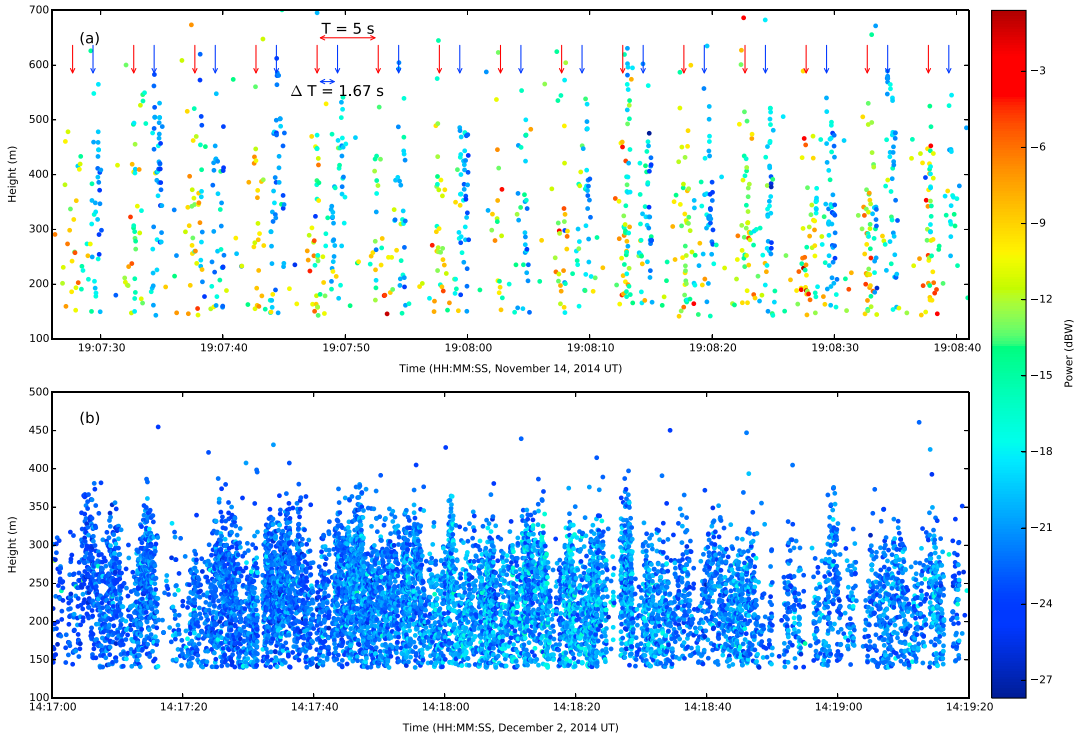

Figure 6. (a) A segment of windmill coronas. Red and blue arrows are both separated by 5 s. The time difference between successive red and blue arrows is 1.67 s. (b) A segment of tower coronas.

so tower coronas do not show such characteristic frequency components. The relationship between these frequency components and the rotation of the windmill will be further analyzed in section 3.2.

4. Tower coronas are usually accompanied by a large negative electric field. This is especially obvious when a large number of lower power (dark blue) sources are produced (19:40–21:40 in Figure 3, 10:30–12:00 and 17:00–21:00 in Figure 4). On the other hand, no special characteristics can be identified for the electric field during the period of windmill coronas. The electric field is usually much weaker and can also be positive when windmill coronas are produced. This indicates that a strong electric field is essential for the production of tower coronas but is not necessary for windmill coronas.

One feature in Figures 3 and 4 that we do not understand is that sources of tower coronas always show an elongated shape oriented in a fixed direction. This should not be due to the network configuration, as sources of windmill coronas do not have such a shape. This should not be due to the influence of the windmill, as the direction is not right to the windmill. This should not be due to the wind effect, as the shape is symmetrical to the tower. This should not be due to some local objects or landforms around the tower, as we made a survey and did not find anything corresponding the orientation. This can be due to some unknown properties of tower coronas, but further observations are needed to make sure that this is not a local phenomenon and is not due to systematic location errors.

3.2. Frequency Analysis for Windmill Coronas

As shown in Figures 3d and 4d, the production of windmill coronas shows three characteristic frequency components, which are apparently related with the rotation of the windmill. However, how these frequency components are related with the windmill rotation is not yet clear.

Figure 6 shows segments of windmill coronas and tower coronas. The production of windmill coronas is apparently periodic, but this is not the case for tower coronas. In Figure 6a, we have drawn some red and blue arrows, both of which are separated by $T = 5$ s, and successive red and blue arrows are separated by $\Delta T = 1.67$ s. T corresponds to $f_1 = 0.2$ Hz in Figure 3d, and $\Delta T = T/3$. It seems that each red arrow corresponds to a column of relatively bright sources, and each blue arrow corresponds to a column of relatively dark sources. We speculate that for one rotation of the windmill, during which the three blades pass the highest point, one blade

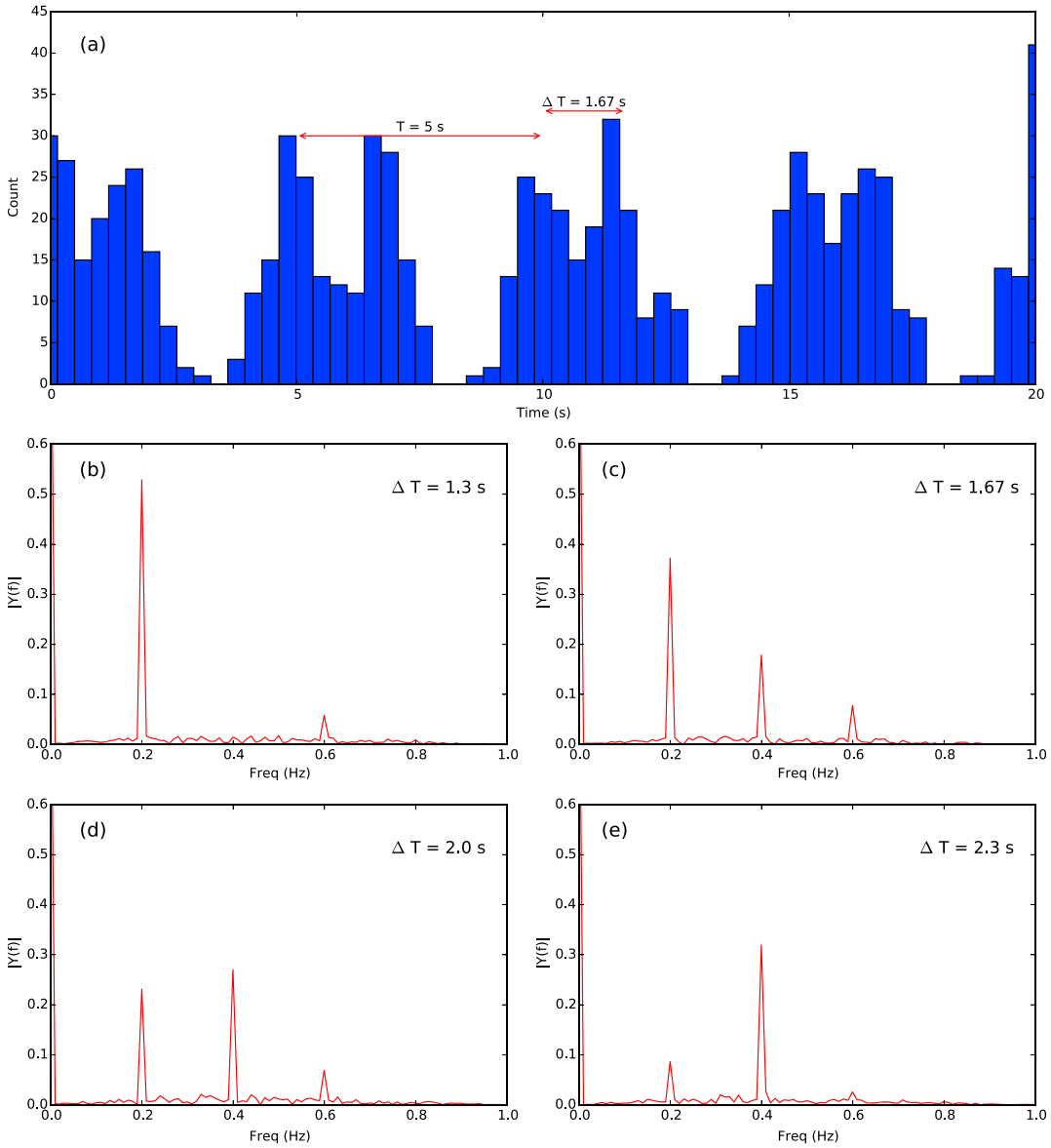

Figure 7. Simulation of the frequency components of windmill corona production. (a) Simulated time series of source numbers. (b–e) Frequency distribution under different values of ΔT.

emits corona discharges relatively strongly, followed by a blade that emits relatively weakly, followed by the third blade having even weaker emissions, which cannot be detected. Then a new rotation with the same behavior follows.

In order to verify this speculation, we did a simple simulation. We simulated a 100 s series of source numbers. At $t_i = 5i$ and $t_j = 5j + \Delta T$ $(i, j = 0, 1, 2, \ldots, 20)$ s, sources with a Gaussian distribution are produced. The probability density for the distribution has the form

$$p(t) = \frac{1}{\sqrt{2\pi\sigma^2}}\left(e^{-\frac{(t-t_i)^2}{2\sigma^2}} + e^{-\frac{(t-t_j)^2}{2\sigma^2}}\right) \quad (1)$$

in which t_i corresponds to the sources produced by the first blade (red arrows in Figure 6a), and t_j corresponds to the sources produced by the second blade (blue arrows in Figure 6a). The parameter σ is the standard deviation of the distribution. We set it as a constant $\sigma = 0.5$ s. We assume that source numbers produced by the two blades have the same distribution. For the case in Figure 6a, $\Delta T = 1.67$ s, and the simulated distribution of source numbers is shown in Figure 7a (only a segment of 0–20 s is shown). The corresponding

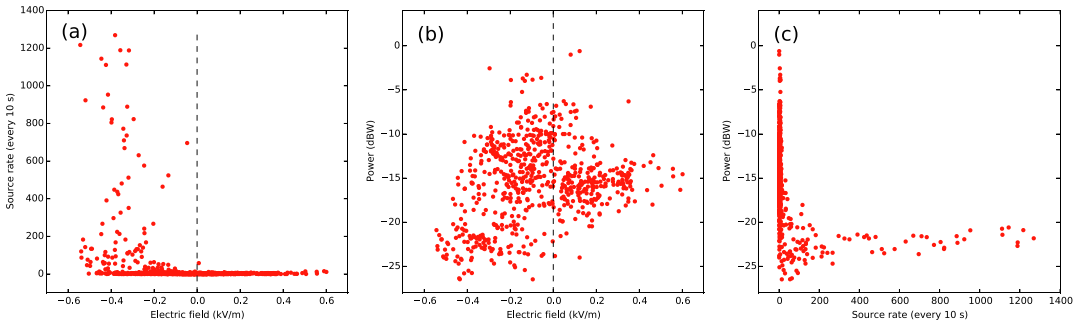

Figure 8. Relationship between some parameters of tower coronas. Shown are scatterplots of (a) the source rate of tower coronas versus the electric field strength, (b) the source power versus the electric field strength, and (c) the source power versus the source rate.

frequency distribution is shown in Figure 7c, which is quite similar to the frequency distribution in Figure 3d. We calculated the frequency distribution with different values of ΔT as shown in Figures 7b–7e. Variation of ΔT causes variations of relative strength of the three frequency components, and it seems that $\Delta T = 1.67$ s gives the most similar result.

With this simulation, we conclude that the three frequency components are indeed caused by corona discharges emitted by two of the three blades, with the first blade emitting relatively strongly and the second relatively weakly. It is likely that the third blade also emits some radiation, which is too weak to be detected though.

We can also calculate the rotation period of the windmill from the frequency components.

$$T = \frac{1}{f_1} \tag{2}$$

For the case in Figure 3, $f_1 = 0.2$ Hz, so the rotation period at that moment was 5 s. For the case in Figure 4, $f_1 = 0.23$ Hz, so the rotation period at that moment was 4.3 s. Although we do not have the data of the windmill rotation period, we know that its rated rotation speed is 11–20 rpm, corresponding to the rotation period of 3–5.5 s, in agreement with our calculations.

Rison et al. [2015] observed corona discharges with a 10-station LMA in a wind farm in Kansas. They found that sources produced from the windmill had the same period as the rotation period of the windmill and concluded that only one of the three blades was producing VHF sources. As the lowest power they could detect was about 10 mW (−20 dBW), higher than that in our study, it is likely that other blades also emitted corona discharges but were too weak to be detected. *Montanya et al.* [2014] also observed corona discharges from a windmill with a 10-station LMA. They observed sources with a period of 3.15 s from the windmill and claimed that this interval "corresponds to the time between each blade tip reaching the highest altitude." This corresponds to a rotation period of 9.45 s for the windmill, which is a relatively long period for a windmill. It also seems that they did not have the data of the actual rotation speed of the windmill. Considering the fact that the power of the corona discharges detected by *Montanya et al.* [2014] was about −5 dBW, it is very likely that *Montanya et al.* [2014] also only detected relatively powerful corona discharges from one blade similar to *Rison et al.* [2015], and 3.15 s is actually the time for one complete rotation of the windmill.

3.3. Relationship Between Tower Coronas and the Electric Field

Characteristics of windmill coronas are controlled by the rotation of the windmill, so it is difficult to study the relationship between their characteristics and other factors such as the electric field. On the other hand, tower coronas do not have such a problem. Besides, tower coronas radiate more weakly, so have not been observed by previous studies. In this section, we will explore the relationship between some characteristics of tower coronas and the electric field. Tower coronas in all selected periods (blue horizontal lines in Figure 1) are analyzed, but periods when the electric field is distorted by lightning flashes are excluded. For every 10 s, source rate, average electric field strength, and average source power are calculated and relations among them are explored.

Figure 8a shows a scatterplot of the source rate of tower coronas versus the electric field strength. Under a positive electric field, the source rate is always very low (below 10 sources per 10 s). Under a relatively strong

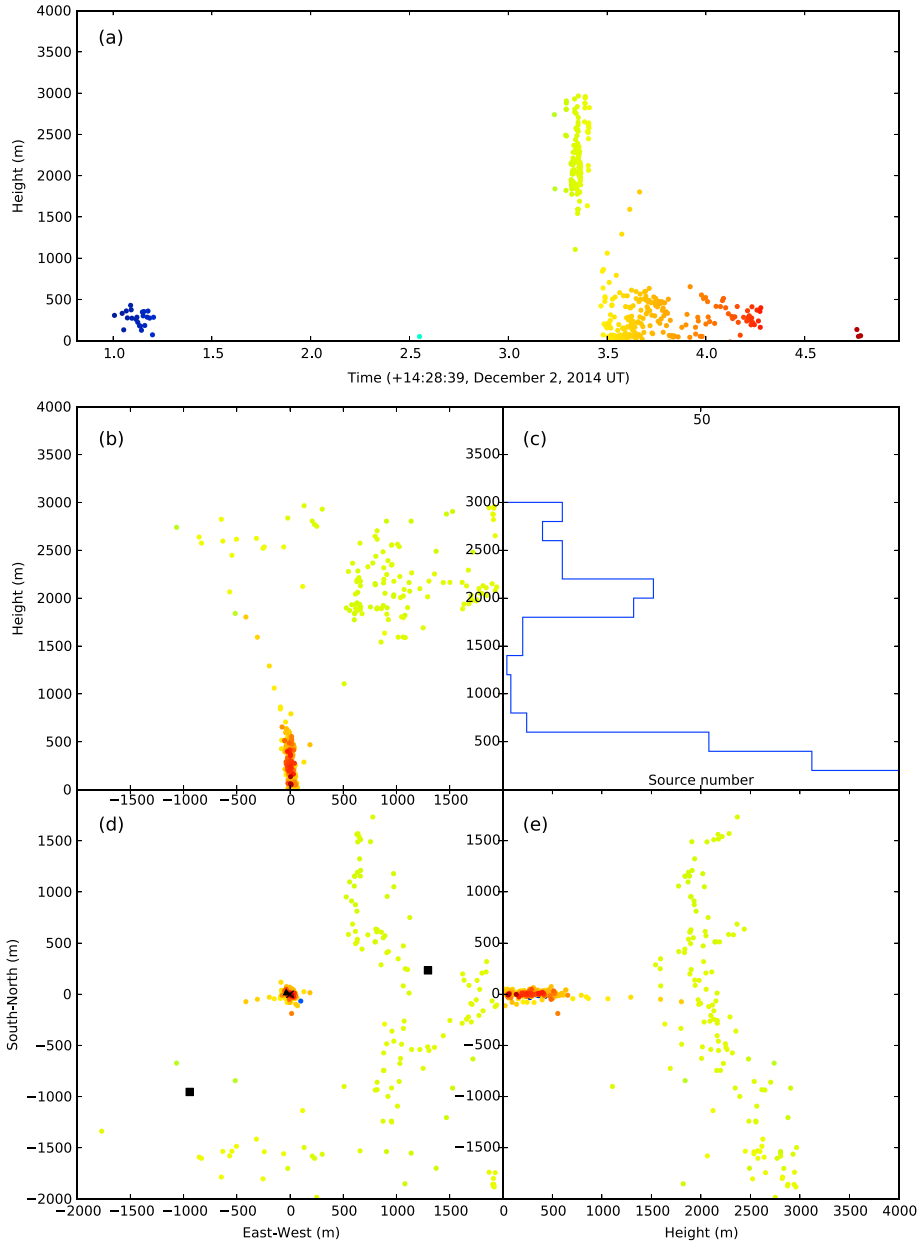

Figure 9. An intracloud flash initiating an aborted upward leader (or just some high-altitude sources of corona discharges, see text). In all views, colors indicate time with the earliest source in blue and the latest source in red.

negative electric field, the source rate can be very high (up to 1000 sources per 10 s). This is consistent with the notion that positive polarity corona discharge is easier to develop [*MacGorman and Rust*, 1998]. However, although it is clear that a large negative electric field is conducive to the production of corona discharges, there is no straightforward relationship between the source rate and the electric field strength. The possible reason is that when the electric field is strong enough and corona discharges frequently occur, the space charges produced by corona discharges will hinder further development of corona discharges even if the electric field gets stronger.

Figure 8b shows a scatterplot of the source power versus the electric field strength. When the electric field is positive, the source power seems to be relatively stable, around −15 dBW, without any clear relationship to the electric field strength. When the electric field is negative, the source power tends to decrease with increasing electric field strength (absolute value). This is somewhat surprising. A related result is shown in Figure 8c, which is a scatterplot of the source power versus the source rate. For sources with powers higher than about

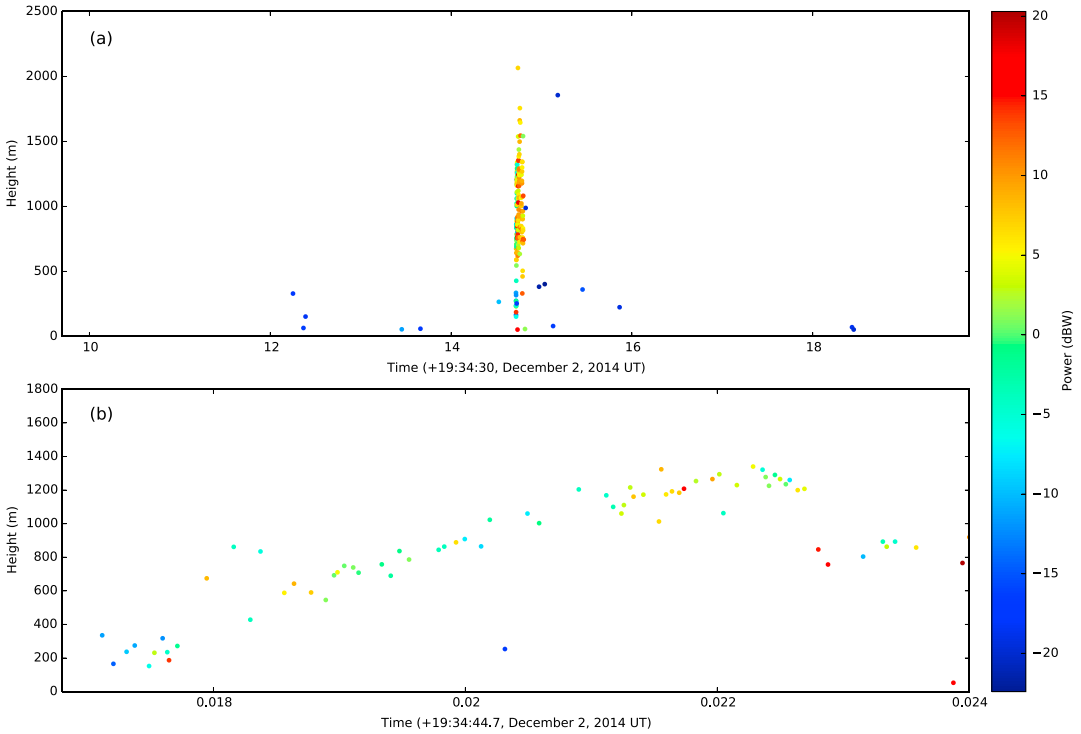

Figure 10. Height-time view of a self-initiated upward lightning from the tower. Color indicates the source power. (a) A section of 5 s before and after the upward lightning. (b) An enlarged view of the upward leader.

−20 dBW, the source rate is usually very low, mostly lower than 10 sources per 10 s. When the source power is below −20 dBW, the source rate can be very high. According to Figure 8a, high source rate corresponds to a strong negative electric field. It seems that only when a strong negative electric field exists can tower coronas occur frequently. However, when a large number of sources are produced, their source powers are always very low. On the other hand, if a positive or a very weak negative electric field exists, tower coronas can rarely occur, but once they occur, their source power tends to be large. This result may also be related with the space charges produced by the corona discharges. High rates of corona discharges produce a significant amount of space charges, which reduce the local electric field and impede the further development of corona discharges, resulting in relatively low source powers.

3.4. Relationship With Lightning Flashes

Windmill coronas are more powerful and possibly develop higher in altitude, so it is expected that they are more likely to initiate lightning flashes. In Figure 3a, there are three upward flashes (F1 – F3) from the tower or the windmill. F1 is close to the end of the most frequent period of windmill coronas. Similarly, in Figure 4a there is one upward flash (F4), which occurred right at the end of a period of frequent windmill coronas. On the contrary, tower coronas do not show any evidence that they may be associated with any lightning flashes. From this respect, windmill coronas seem to be more likely to precede lightning flashes. However, F1 in Figure 3a is at least tens of seconds apart from the most frequent corona discharges. In other words, the activity of windmill coronas has already diminished before the onset of the flash. For F4 in Figure 4a, a close look at its LMA sources shows that there is an intracloud flash near the windmill initiating an aborted upward leader from the windmill as shown in Figure 9. We can see that an intracloud flash occurred around the tower and windmill, and less than 0.1 s after, an upward leader was initiated. The leader propagated to nearly 2000 m altitude and then stopped. This kind of other-triggered upward leader is commonly observed in winter [*Wang et al.*, 2008], and there is no evidence that the intracloud flash has any connection with the corona discharges before it. It is also possible that the aborted upward leader is actually some relatively high sources of corona discharges, according to the time scale. Either way, we found no direct evidence that either windmill coronas or tower coronas are associated with the initiation of lightning flashes.

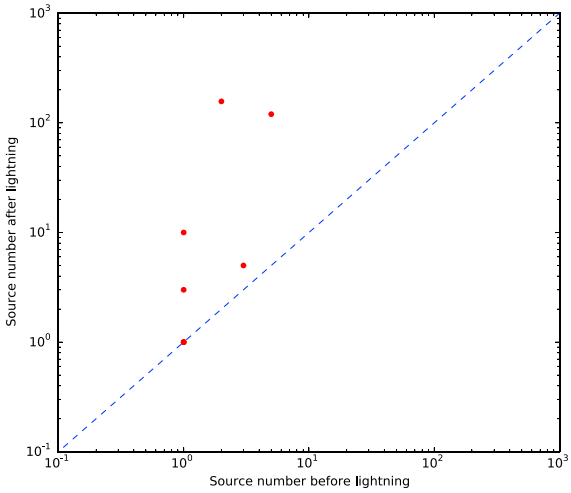

Figure 11. Source numbers of corona discharges within 2 s before and after nearby lightning flashes.

In fact, all of the above flashes (F1–F4) are other-triggered upward flashes [*Wang et al.*, 2008; *Saba et al.*, 2016]. Such flashes are initiated by a rapid electric field change caused by other nearby lightning flashes, so it is an expected result that they do not have any relationship with corona discharges. In winter, self-triggered upward lightning flashes are also commonly observed [*Wang et al.*, 2008]. These flashes are caused by a slowly built up background electric field. During the period of the analysis for this study, there are three self-triggered upward flashes, but still, we cannot find any evidence that they are related with preceding corona discharges. One example is shown in Figure 10. Figure 10a shows a section of 5 s before and after the upward flash. We can see there are only five sources within 5 s before the flash, an extremely low source rate as compared with Figure 8a. Therefore, the preceding corona discharges do not seem to have any influence on the upward flash.

On the other hand, lightning discharges nearby should be able to influence the space charges and the local electric field, so it is expected that lightning discharges may have certain impact on corona discharges. The case in Figure 9 shows such a feature. There are few corona discharges within about 2 s before the intracloud flash, but right after it, numerous sources of corona discharges are detected, and they develop higher than those before the intracloud flash. It seems that the intracloud flash is capable of generating a burst of corona discharges. Figure 11 shows the relationship between source numbers of corona discharges 2 s before and 2 s after lightning flashes within 5 km of the windmill. Cases with the source number of zero are not plotted in the figure. We can see that for most cases, the source number of corona discharges after a flash is larger than that before a flash. Note that the axes are logarithmic scales, so there are usually far more sources within 2 s after a flash than within 2 s before a flash. This result indicates that a lightning flash near a tall object is indeed able to increase the rate of corona discharges from the tall object right after the flash. This is probably due to the abrupt and large variation of the electric field at the tip of the tall object caused by the lightning flash.

4. Discussion

4.1. Production Frequency of Windmill Coronas

The differences between windmill coronas and tower coronas are mainly caused by the periodic rotation of the windmill. For a stationary object, the space charges produced by the corona discharges can reduce the electric field at the tip of the object and suppress the further development of corona discharges. For windmills, however, the moving blades can get rid of the space charges produced by corona discharges and the electric field at the tips of the blades can be sustained, so windmill coronas are more powerful than tower coronas.

One mystery about the windmill corona is its production frequency. In section 3.2, we have demonstrated that for one rotation of the windmill, during which three blades pass the highest point, corona discharges from the first blade have the largest power (strong radiation), those from the second blade have relatively weak power (medium radiation), and those from the third blade have even weaker power, which could not be detected (weak radiation) (Figure 6a). This scenario is illustrated in Figure 12a. The observations by *Rison et al.* [2015] and *Montanya et al.* [2014] showed different phenomena, but as demonstrated in section 3.2, it is possible that they actually only detected the relatively strong radiation from the first blade. The problem here is that if the three blades are exactly the same, it is unclear why the variation period of the radiation power has to be the same as the rotation period of the windmill. Instead of the observed pattern (Figure 12a), it should be equally possible to be strong to medium+ to medium− to weak and back to strong (Figure 12b), or strong to medium to weak to medium and back to strong (Figure 12c), and the period for corona discharge production would be four thirds of the rotation period. The fact that only the first scenario has been observed in different regions of the world indicates that there are some fundamental mechanisms behind this phenomenon.

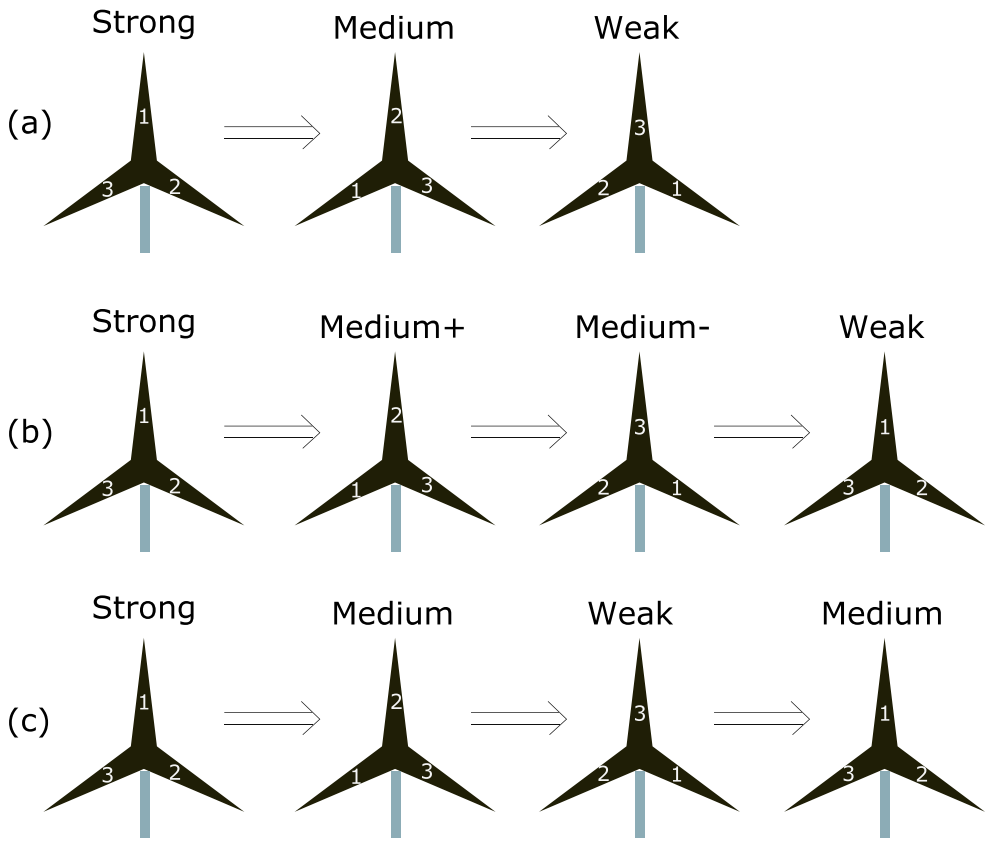

Figure 12. Illustration of three possible scenarios of one period of corona discharge production on the windmill. (a) A scenario that has been observed. (b, c) Scenarios that should also be possible if the three blades of the windmill are the same.

One possible explanation may be related with the production and drifting away of space charges produced by corona discharges. On the first blade, powerful corona discharges produce a large amount of space charges. These charges drift away slowly in the ambient electric field. Corona discharges on the second blade are weaker due to the space charges. At this stage, the space charge density is still increasing, which makes corona discharges on the third blade even weaker. Extremely weak corona discharges result in a rapid decrease of the space charge density, so corona discharges on the next blade become powerful again.

In the case of a tower, the production and drifting away of the space charges can reach an equilibrium so the power of tower coronas is relatively stable. For the case of a windmill, the fast moving blade can get rid of the space charges and produce more powerful radiation, which results in the higher density of space charges and makes the subsequent blade produce less powerful radiation. As a result, the radiation power of windmill coronas shows periodic fluctuations.

However, it is still difficult to explain why the scenarios in Figures 12b and 12c cannot happen. The time constants for the production and drifting away of space charges must satisfy certain relationships with the rotation period of the windmill to make it only possible for the scenario in Figure 12a.

Another possible explanation that is much simpler is that one of the three blades has developed an imperfection as suggested by *Rison et al.* [2015]. The imperfect blade can always produce relatively powerful radiation so the variation period of the radiation power is always the same as the rotation period. Considering the fact that windmills are frequently struck by lightning, imperfections on any blade is possible. However, it is still difficult to explain the observation in our study that at least two blades produce corona discharges. We can consider that two of the three blades of the windmill in our study have developed imperfections. The second blade produced relatively weak radiation due to the space charges produced by the first blade. However, for a wind farm as in the study of *Rison et al.* [2015] and *Montanya et al.* [2014], windmills with imperfections on

one, two, or even three blades should all exist, and different patterns of the variation of radiation power should have been detected; but apparently, only one pattern has been observed by *Rison et al.* [2015] and *Montanya et al.* [2014].

It would be interesting to know what would happen if the windmill rotated much more slowly or much more rapidly and what would happen if the windmill had four or more blades. Further observation and simulation works are needed to answer these questions.

4.2. Source Height of Corona Discharges

As shown in Figures 2 and 5b, the source height distributions of both windmill coronas and tower coronas peak at around 250 m. Altitudes of the windmill and the tower are 150 m and 155 m above mean sea level. It seems that most corona discharges occur about 100 m above the top of the windmill and the top of the tower. This is in disagreement with the observation by *Rison et al.* [2015] which showed that most sources were located between the hub and the blades of the windmill.

Figure 5b also shows that the source height of windmill coronas has a much wider distribution extending higher in the sky than that of tower coronas. They have a difference of about 100 m on the average source height.

One possible reason for these results is that corona discharges observed in this study include streamers emanating from the windmill and/or the tower and dying out several hundred meters above. Streamers from the windmill carry larger energy and can develop higher above. For the case in Figure 9, if we consider the several upward propagating sources after the intracloud flash as produced by corona discharges, it is evident that corona discharges can develop upward propagations after an abrupt electric field change. It is possible that corona discharges observed by *Rison et al.* [2015] are the so-called "glow corona" without any streamers developing upward [e.g., *Becerra*, 2013].

Another piece of evidence for this speculation is the source power. The source power of corona discharges, especially windmill coronas, observed in this study seems to be close to that of the initial portion of upward leaders. Figure 10b shows the first 17 ms of a self-initiated leader from the tower. The first several sources have powers of about −10 dBW, close to the typical source power of windmill coronas (Figure 5a). As the leader develops upward, the source power gets much larger.

Corona discharges can consist of both electrical avalanches and streamer processes [*Cooray*, 2015], and it is possible that a significant portion of the sources observed in this study are produced by streamer processes. Sources of the electrical avalanches may have even lower power and were not detected, or they may be the low tail in the source power distribution (Figure 5).

However, one difficulty for this explanation is that there is no observational evidence that streamers near the sea level can develop for more than 100 m. It is also possible that the location error is the reason for the height distributions and differences between windmill and tower coronas.

The estimated height error is given by the following relation [*Thomas et al.*, 2004]:

$$\Delta z \simeq c\Delta t \left(\frac{d+r}{z}\right) \tag{3}$$

where c is the speed of light, Δt is the timing error, z is the source height above the ground, d is the horizontal distance between the source and the closest station, and r is the slant distance. The timing error is assumed to be the same as the timing error of GPS: $\Delta t \simeq 40$ ns. In our case, the closest site is about 1430 m from the windmill and the tower, and the source height is assumed to be the same as the top of the windmill and the top of the tower (height above the ground), so $d \simeq 1430$ m, $r \simeq 1433$ m, and $z \simeq 100$ m. This gives us $\Delta z \simeq 344$ m. This height error is relatively large compared with the error for normal lightning discharges due to the fact that corona discharges occur near the ground. This error may account for the 100 m difference between the peaks of height distributions in Figure 2 and the top heights of the windmill and the tower.

The location error may also be the reason for the difference of height distributions of windmill and tower coronas in Figure 5b. As shown in Figure 5c, the distribution of χ_v^2 is wider for windmill coronas, indicating that location results of windmill coronas have larger errors. As one reviewer suggested, windmill coronas may produce pulses with higher powers and longer durations. The longer duration makes a larger timing error Δt, and thus a larger height error Δz for windmill coronas.

5. Conclusions

Observations of corona discharges from a windmill and its lightning protection tower with a nine-station LMA are reported. Because of the moving blades capable of escaping shielding space charges, windmill coronas are distinctly different from tower coronas. Windmill coronas generally have larger powers and possibly develop higher upward than tower coronas do. The average source powers are −15.5 and −21.7 dBW, and average source altitudes 321.0 and 230.5 m, respectively, for windmill coronas and tower coronas. Tower coronas tend to be produced in a strong negative electric field, but windmill coronas do not have a clear relationship with the electric field.

The source production of windmill coronas shows three frequency components: f_1, f_2, and f_3, in which $f_2 = 2f_1$ and $f_3 = 3f_1$. These frequency components are caused by the periodic rotation of the windmill, so they do not exist for tower coronas. Close examination of the time series of sources of windmill coronas and a simple simulation showed that during one rotation of the windmill, in which three blades pass the highest point, the first blade produces sources with large power, the second blade produces sources with median power, and the third blade produces sources with weak power which cannot be detected. The reason for such periodic variation is still not clear.

The relationship between tower coronas and the background electric field is investigated. Under a positive or weak negative electric field, the source rate of tower coronas is always very low (below 10 sources per 10 s). Under a strong negative electric field, the source rate can sometimes be very high (up to 1000 sources per 10 s). The source rate of tower coronas is also related with the source power. Only when the source power is lower than about −20 dBW can the source rate get very high. For sources with powers higher than about −20 dBW, source rates are mostly lower than 10 sources per 10 s.

The relationship between corona discharges and lightning flashes is also investigated. We did not find any direct evidence that either type of corona discharge raises the chance of upward leader initiation. But lightning flashes near the windmill and the tower can increase the production rate of corona discharges right after the flashes.

Source altitudes of corona discharges in this study are on average about 100 m higher than the top of the windmill and the top of the tower. We speculate that a significant portion of corona discharge sources observed in this study are produced by streamer processes. However, this explanation also has some difficulties, and another possible reason is that the location error caused this result. The estimated height error for corona discharges is 344 m, which is relatively large due to low source altitudes of corona discharges. The height difference between windmill coronas and tower coronas may also be due to the location error.

Acknowledgments

The data for this paper were obtained during the winter campaign in 2014. Readers can request the data from the corresponding author (tingwu@gifu-u.ac.jp). This work was supported by the Ministry of Education,Culture, Sports, Science, and Technology of Japan (grant 2336012) and Japan Power Academy Special Research 2013.

References

Becerra, M., V. Cooray, S. Soula, and S. Chauzy (2007), Effect of the space charge layer created by corona at ground level on the inception of upward lightning leaders from tall towers, *J. Geophys. Res.*, *112*, D12205, doi:10.1029/2006JD008308.

Becerra, M. (2013), Glow corona generation and streamer inception at the tip of grounded objects during thunderstorms: Revisited, *J. Phys. D: Appl. Phys.*, *46*, 135205, doi:10.1088/0022-3727/46/13/135205.

Brook, M. (1992), Breakdown electric fields in winter storms, *Res. Lett. Atmos. Electr.*, *12*, 47–52.

Cooray, V. (2015), *An Introduction to Lightning*, pp. 7–19, Springer, Netherlands.

MacGorman, D. R., and W. D. Rust (1998), *The Electrical Nature of Storms*, vol. 78, Oxford Univ. Press, New York.

Montanya, J., O. van der Velde, and E. R. Williams (2014), Lightning discharges produced by wind turbines, *J. Geophys. Res. Atmos.*, *119*, 1455–1462, doi:10.1002/2013JD020225.

Narita, K., Y. Goto, H. Komuro, and S. Sawada (1989), Bipolar lightning in winter at Maki, Japan, *J. Geophys. Res.*, *94*(D11), 13,191–13,195, doi:10.1029/JD094iD11p13191.

Rison, W., R. J. Thomas, P. R. Krehbiel, T. Hamlin, and J. Harlin (1999), A GPS-based three-dimensional lightning mapping system: Initial observations in central New Mexico, *Geophys. Res. Lett.*, *26*, 3573–357.

Rison, W., K. Cummins, R. Thomas, P. Krehbiel, D. Rodeheffer, M. Quick, and J. Myers (2015), Observations of corona discharges from wind turbines, in *International Conference on Lightning and Static Electricity*, pp. 48–55, IET Digital Library, Toulouse, France, doi:10.1049/ic.2015.0195.

Saba, M. M., C. Schumann, T. A. Warner, M. A. S. Ferro, A. R. de Paiva, J. Helsdon Jr., and R. E. Orville (2016), Upward lightning flashes characteristics from high-speed videos, *J. Geophys. Res. Atmos.*, *121*, 8493–8505, doi:10.1002/2016JD025137.

Soula, S., and S. Chauzy (1991), Multilevel measurement of the electric field underneath a thundercloud: 2. Dynamical evolution of a ground space charge layer, *J. Geophys. Res.*, *96*(D12), 22,327–22,336, doi:10.1029/91JD02032.

Standler, R. B., and W. P. Winn (1979), Effects of coronae on electric fields beneath thunderstorms, *Q. J. R. Meteorol. Soc.*, *105*, 285–302, doi:10.1002/qj.49710544319.

Takeuti, T., M. Nakano, M. Brook, D. J. Raymond, and P. Krehbiel (1978), The anomalous winter thunderstorms of the Hokuriku Coast, *J. Geophys. Res.*, *83*(C5), 2385–2394, doi:10.1029/JC083iC05p02385.

Thomas, R. J., P. R. Krehbiel, W. Rison, T. Hamlin, J. Harlin, and D. Shown (2001), Observations of VHF source powers radiated by lightning, *Geophys. Res. Lett.*, *28*(1), 143–146, doi:10.1029/2000GL011464.

Thomas, R. J., P. R. Krehbiel, W. Rison, S. J. Hunyady, W. P. Winn, T. Hamlin, and J. Harlin (2004), Accuracy of the lightning mapping array, *J. Geophys. Res.*, *109*, D14207, doi:10.1029/2004JD004549.

Toland, R. B., and B. Vonnegut (1977), Measurement of maximum electric field intensities over water during thunderstorms, *J. Geophys. Res.*, *82*(3), 438–440, doi:10.1029/JC082i003p00438.

Wang, D., N. Takagi, T. Watanabe, H. Sakurano, and M. Hashimoto (2008), Observed characteristics of upward leaders that are initiated from a windmill and its lightning protection tower, *Geophys. Res. Lett.*, *35*, L02803, doi:10.1029/2007GL032136.

Wang, D., and N. Takagi (2012), Characteristics of winter lightning that occurred on a windmill and its lightning protection tower in Japan, *IEEJ Trans. Power Energy*, *132*(6), 568–572, doi:10.1541/ieejpes.132.568.

Wang, D., W. Rison, N. Takagi, R. J. Thomas, H. E. Edens, D. Rodeheffer, and P. R. Krehbiel (2015), Japan winter upward lightning: Triggering source, initial leader progression and parent storm charge structure, in *Proceedings of 9th Asia-Pacific International Conference on Lightning*, pp. 1–3.

Waters, R. T. (1975), Characteristics of the stabilized glow discharge in air, *J. Phys. D: Appl. Phys.*, *8*, 416–426.

Wu, T., Y. Takayanagi, T. Funaki, S. Yoshida, T. Ushio, Z. Kawasaki, T. Morimoto, and M. Shimizu (2013), Preliminary breakdown pulses of cloud-to-ground lightning in winter thunderstorms in Japan, *J. Atmos. Sol. Terr. Phys.*, *102*, 91–98, doi:10.1016/j.jastp.2013.05.014.

Wu, T., S. Yoshida, T. Ushio, Z. Kawasaki, Y. Takayanagi, and D. Wang (2014), Large bipolar lightning discharge events in winter thunderstorms in Japan, *J. Geophys. Res. Atmos.*, *119*, 555–566, doi:10.1002/2013JD020369.

Erratum

In the originally published version of this article, the height units in Figure 9 and Figure 10 should read 'm' instead of 'km'. The error has since been corrected and this version may be considered the authoritative version of record.